Atmos. Chem. Phys. Discuss., doi:10.5194/acp-2016-489, 2016
Manuscript under review for journal Atmos. Chem. Phys.
Published: 1 July 2016

Constraining the ship contribution to the aerosol of the Central Mediterranean

S. Becagli[1], F. Anello[2], C. Bommarito[2], F. Cassola[3,4], G. Calzolai[5], T. Di Iorio[6], A. di Sarra[6], J.L. Gómez-Amo[6,7], F. Lucarelli[5], M. Marconi[1], D. Meloni[6], F. Monteleone[2], S. Nava[5], G. Pace[6], M. Severi[1], D. M. Sferlazzo[8], R. Traversi[1], and R. Udisti[1]

[1] Department of Chemistry, University of Florence, Sesto Fiorentino, Florence, I-50019, Italy
[2]ENEA, Laboratory for Earth Observations and Analyses, Palermo, I-90141, Italy
[3]Department of Physics & INFN, University of Genoa, Genoa, I-16146, Italy.
[4]ARPAL-Unità Operativa CFMI-PC, Genova, I-16129, Italy.
[5]Department of Physics, University of Florence & INFN-Firenze, Sesto Fiorentino, Florence, I-50019, Italy.
[6]ENEA Laboratory for Earth Observations and Analyses, Roma, I-00123, Italy
[7]Department of Earth Physics and Thermodynamics, University of Valencia, Spain.
[8]ENEA, Laboratory for Earth Observation and Analyses, Lampedusa, I-92010, Italy

Keywords: ship aerosol, Central Mediterranean Sea, PM_{10}, La-Ce ratio, Vanadium.

Abstract

PM_{10} aerosol samples were collected during summer 2013 within the framework of the Chemistry and Aerosol Mediterranean Experiment (ChArMEx) at two sites located North (Capo Granitola, 36.6°N, 12.6°E) and South (Lampedusa Island, 35.5°N, 12.6°E), respectively, of the main Mediterranean shipping route in the Sicily Channel.
The PM_{10} samples were collected with 12 hour time resolution at both sites. Selected metals, main anions, cations, and elemental and organic carbon were determined.
The evolution of soluble V and Ni concentrations (typical markers of heavy fuel oil combustion) was related to meteorology and ship traffic intensity in the Sicily Channel, using a high resolution regional model for back trajectories calculation. Elevated concentration of V and Ni were associated with transport from the Sicily Channel and coincidences between trajectories and positions of large ships, both at Capo Granitola and Lampedusa; the vertical structure of the planetary boundary layer also appears to play a role, with high V values associated with strong inversions and stable boundary layer. The V concentration was generally lower at Lampedusa than at Capo Granitola, where it reached a peak value of 40 ng/m^3.
Concentrations of rare earth elements, La and Ce in particular, were used to identify possible contributions from refineries, whose emissions are also characterized by elevated V and Ni amounts; refinery emissions are expected to display high La/Ce and La/V ratios, due to the use of La in the fluid catalytic converter systems. In general, low La/Ce and La/V ratios were observed in the PM samples, allowing to unambiguously identify the large role of the ship source in the Sicily Channel.

Based on the sampled aerosols, ratios of the main aerosol species arising from ship emission with respect to V were estimated with the aim of deriving a lower limit for the total ship contribution to PM_{10}. The estimated minimum ship emission contributions to PM_{10} was 1.9 $\mu g/m^3$ at Lampedusa, and 2.8 $\mu g/m^3$ at Capo Granitola, corresponding to 11% and 8.2% of PM_{10}, respectively.

1. Introduction

Ship emissions may significantly affect atmospheric concentrations of several important pollutants, especially in maritime and coastal areas (e.g. Endresen et al., 2003). Main emitted compounds are carbon dioxide (CO_2), nitrogen oxides (NO_x), sulfur dioxide (SO_2), carbon monoxide (CO), hydrocarbons, and primary and secondary particles. Thus, ship emissions impact the greenhouse gas budget (Stern, 2007), acid rain (through NO_x and SO_2 oxidation products; Derwent at al., 2005), human health (CO, hydrocarbons, particles; Lloyd's Register Engineering Services, 1995; Corbett et al., 2007) and solar radiation budget through aerosol direct and indirect effects (black carbon and sulfur containing particles; Devasthale et al., 2006; Lauer et al., 2007; Coakley and Walsh, 2002).
Heavy oil fuels used by ships contain varying transition metals originating from the fuel. The aerosol emitted by ship engines is formed at high temperature (>800°C) from V, Ni, Fe compounds (Sippula et al., 2009). The thermodynamics predict that these species mainly form oxides, but when the flue gas dew point is reached, sulfuric acid (which was found to form a liquid layer on the ultra-fine particles) condenses on it leading to partial dissolution of the ultra-fine seeds, probably increasing the toxicity of the particles when inhaled.
In spite of the great amount of gas and particulate arising from ship emission, maritime transport is relatively clean if calculated per kilogram of transported material, and it is currently increasing with respect to air and road transport (Micco and Pérez, 2001; Grewal and Haugstetter, 2007). In addition, emissions from other transport sectors are decreasing due to the implementation of advanced emission reduction technologies, and the relative impact of shipping emissions is increasing.
Regulations aiming at reducing emissions based on restrictions on the fuel sulfur content (sulfur emission control areas, SECAs) have been implemented in several regions. Although the legislation is focussed on sulfur emissions, the overall health and environmental effects of the emissions depend in a complicated manner on the physical and chemical properties of the emissions (WHO, 2013). Several studies have been carried out to determine the detailed chemical composition of shipping emissions (Agrawal et al., 2008a and b, Moldanová et al., 2009, Murphy et al., 2009, Lyyränen et al 1999, Cooper, 2003, Sippula et al. 2014); however, in comparison to on-road vehicles, the ships emissions are still poorly characterized.
A large variety of anthropic sources (refineries, power plants, intense ship traffic), also associated with a high population density, and natural emissions make the

Mediterranean region one of the most polluted in the world (e.g., Kouvarakis et al., 2000; Marmer and Langmann, 2005). This multiplicity of Mediterranean sources (some of which with the same markers of ship aerosol) makes difficult the quantification of ship contribution to the total aerosol amount (e.g., Becagli et al., 2012).

The contribution of ships and harbour emissions to local air quality, with specific focus on atmospheric aerosol, has been investigated using models (Trozzi et al., 1995; Gariazzo et al., 2007; Eyring et al., 2005; Marmer et al., 2009), experimental analyses at high temporal resolution (Ault et al., 2010; Contini et al., 2011; Jonsson et al., 2011; Diesch et al., 2013; Donateo et al., 2014), receptor models based on identification of chemical tracers associated with ship emissions (Viana et al., 2009; Pandolfi et al., 2011; Cesari et al., 2014), and integrated approaches with receptor and chemical transport models (Bove et al., 2014). Few studies exist in open sea (Becagli et al., 2012; Schembari et al., 2014; Bove et al., 2016).

In this context, studies performed at Mediterranean sites, where it is possible to distinguish ship emission from other sources of heavy fuel oil combustion, are important to investigate the current impact of the ship emissions on primary and secondary aerosols. In a previous study (Becagli et al., 2012) we used measurements of PM_{10} and relative chemical composition carried out at Lampedusa, in the central Mediterranean, to investigate the role of ship emissions. Vanadium and Nickel were used as tracers of heavy fuel combustion together with trajectory analyses to assess the role of ship traffic. The ship source, however, could not be unequivocally separated from possible influences from refineries and power plants, which use similar fuels. In summer 2013 we addressed the same topic by implementing a specific strategy to target the aerosols due to ship emissions. PM_{10} samples were collected in parallel at Lampedusa (LMP) and at Capo Granitola (CGR), i.e., respectively South and North of the main shipping route through the Mediterranean, with the aim of isolating the ship source. Figure 1 shows the map of the measurement stations in the central Mediterranean; Capo Granitola is about 230 km North of Lampedusa. The analysis is complemented with measurements of Rare Earth Elements (REEs), trajectories from a high resolution regional model, and actual observations of ship traffic. The combination of these approaches allows unambiguously identifying and providing constraints for the ship contribution to PM_{10} in the central Mediterranean.

The PM_{10} samples were collected in summer 2013 as a contribution to the Chemistry and Aerosol Mediterranean Experiment (ChArMEx; http://charmex.lsce.ispl.fr). Lampedusa is one of the supersites of the ChArMEx experiment; a list of the instruments deployed during the special observing period 1a of ChArMEx, and of the measurement strategy, meteorological conditions, and main observations is given by Mallet et al. (2016).

Atmos. Chem. Phys. Discuss., doi:10.5194/acp-2016-489, 2016
Manuscript under review for journal Atmos. Chem. Phys.
Published: 1 July 2016

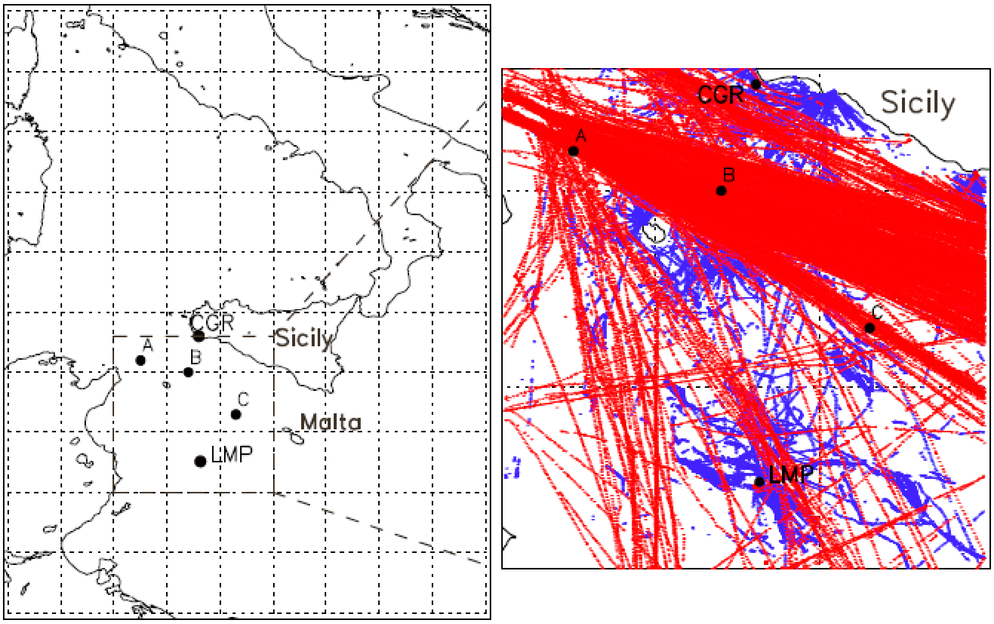

Figure 1. Map of the study area with the sites of Lampedusa (LMP) and Capo Granitola (CGR) (left panel). A, B and C indicate the three sites selected to study the stability of the boundary layer in the Sicily Channel (see section 3.2.2). The ship routes in the study area during the first 10 days of June 2013 are displayed in the right panel. Red and blue dots show the routes of merchant and fishing vessels, respectively.

2. Measurements and methods

2.1. Aerosol sampling and chemical analyses

PM_{10} was sampled at two sites: at the Station for Climate Observations, maintained by ENEA (the Italian Agency for New Technologies, Energy, and Sustainable Economic Development) on the island of Lampedusa (35.5°N, 12.6°E), and at the Italian CNR (National Research Council) Research Centre at Capo Granitola (36.6°N, 12.6° E). Lampedusa is a small island in the Central Mediterranean sea, more than 100 km far from the nearest Tunisian coast. At the Station for Climate Observations, which is located on a 45 m a.s.l. plateau on the North-Eastern coast of Lampedusa, continuous observations of greenhouse gases concentration (Artuso et al., 2007, 2009), aerosol properties (di Sarra et al., 2011, 2015; Becagli et al., 2013; Marconi et al., 2014; Calzolai et al., 2015), total ozone, ultraviolet irradiance (Meloni et al., 2005), solar and infrared radiation (di Sarra et al., 2011; Meloni et al., 2012, 2015), and other climatic parameters are carried out.

PM_{10} is routinely sampled on a daily basis at LMP (Becagli et al., 2013; Marconi et al., 2014; Calzolai et al., 2015). For the intensive ChArMEx campaign, samples were collected from 1 June to 3 August at 12-hour resolution by using a low volume dual channel sequential sampler (HYDRA FAI Instruments) equipped with two PM_{10} sampling heads operating in accord with UNI EN12341.
The two channels operated in parallel and were loaded with different types of filters: the first one with 47 mm diameter, 2 μm nominal porosity Teflon filters, for ion chromatographic analysis of soluble ions, atomic emission spectroscopy for soluble metals, and proton-induced X-ray emission (PIXE) for the total (soluble+insoluble) elemental composition; the second one with 47 mm pre-fired, 2 μm nominal porosity, quartz filters for elemental (EC) and organic carbon (OC) determinations.
The sampling site at CGR is located at Torretta Granitola, a Research Center of the Italian National Research Council, in South-Western Sicily (12 km from Mazara del Vallo). The sampler was installed on the roof of one of the research centre buildings at about 20 m a.s.l., directly on the coastline, facing the strait of Sicily.
At CGR PM_{10} samples were collected at 12 hour resolution with a TECORA Skypost sequential sampler on 47 mm pre-fired, 2 μm nominal porosity, quartz filters allowing the determination of ions, metals, EC and OC on different fractions of the filter. Due to technical problems, some diurnal samplings were lost at CGR.

The PM_{10} mass was determined by weighting the filters before and after sampling with an analytical balance in controlled conditions of temperature (20±1 °C) and relative humidity (50±5 %). The estimated error on PM_{10} mass is around 1% at 30 $\mu g/m^3$ in the applied sampling conditions.
A quarter of each Teflon filter from LMP and a 1.5x1 cm punch of the quartz filter from CGR were analysed by Ion Chromatography (IC) in the analytical conditions described in Marconi et al. (2014). The estimated uncertainty for IC measurements is 5% for all the considered ions.
Blank values were negligible with respect to the concentration in the samples for Teflon filters. Blank values for quartz filters were negligible for most of the analyzed species, and when not negligible, anyway lower than 25th percentile, they were subtracted from the measured concentrations.
Another quarter of the Teflon filter from LMP, and another 1.5x1 cm punch of the quartz filter from CGR were extracted in ultrasonic bath for 15 min with MilliQ water acidified at pH 1.5–2 with ultrapure HNO_3 obtained by sub-boiling distillation. This extract was used for the determination of the metals soluble part by means of an Inductively Coupled Plasma Atomic Emission Spectrometer (ICP-AES, Varian 720-ES) equipped with an ultrasonic nebulizer (U5000 AT+, Cetac Technologies Inc.). The chosen value of pH is the lowest found in rainwater (Li and Aneja, 1992) and leads to the determination of the metals fraction available to biological organisms and, for some metals (e.g. V and Ni), related to the anthropic source (Becagli et al., 2012).
The remaining half Teflon filter from Lampedusa was analysed by proton induced X ray emission (PIXE) technique (Lucarelli et al., 2011). PIXE analysis is a non-destructive

method for metals. Thus, after the PIXE analysis, this part of the Teflon filter and another punch of the quartz filter from CGR were used for the determination of metals by ICP-AES through the solubilisation procedure according with the method reported in the EU EN14902 (2005) rule, by using concentrated sub-boiling distilled HNO_3 and 30% ultrapure H_2O_2 in a microwave oven at 220°C for 25 min (P = 55 bar). Although this solubilisation procedure is not able to completely dissolve the silicate species, is able to recover at least 70% of the same elements measured by PIXE also for elements having dominant crustal source (unpublished data) due to the low crustal aerosol load in these sampling period (e.g., Mailler et al., 2016).
The OC and EC measurements were carried out on a 1.5x1 cm punch of the quartz filters from Lampedusa and Capo Granitola by means of a Sunset thermo-optical transmittance analyser, following the NIOSH protocol (Wu et al, 2016).

2.3. Atmospheric model and trajectory calculations

Numerical simulations with a non-hydrostatic mesoscale atmospheric model were used to characterize the meteorological conditions in the Sicily Channel during the campaign and to support the interpretation of the experimental results. The Weather Research and Forecasting (WRF) model (Skamarock et al., 2008) outputs, provided by the Department of Physics of the University of Genoa, Italy, were used, covering the entire Mediterranean with a grid spacing of 10 km and hourly temporal resolution. Initial and boundary conditions to drive WRF simulations are obtained from the Global Forecast System operational global model (Environmental Modeling Center, 2003) outputs (0.5x0.5 square degree). Some recent applications of the modelling chain are described in Mentaschi et al. (2015) and Cassola et al. (2016), where full details on the model configuration can also be found.
In particular, the WRF 3-D hourly meteorological fields were used to perform a backward trajectory analysis with the NOAA HYbrid Single-Particle Lagrangian Integrated Trajectory Model (HYSPLIT; Stein et al. 2015), aimed at assessing the origin of air masses impacting the monitoring sites and at supporting the source attribution suggested by the analysis of specific markers (see, in particular, Section 3.2.2). The use of a high-resolution regional atmospheric model for trajectory calculations allows a better representation of boundary layer properties and mesoscale phenomena such as land/sea breezes, which can have a relevant impact especially in complex topography coastal sites like CGR.
Specifically, 48-h long back trajectories were computed at each site from a reference height of 10 m above ground level, starting every six hours for the whole period of the campaign, from 10th June to 31st July 2013.

2.4. Ships/marine traffic

Atmos. Chem. Phys. Discuss., doi:10.5194/acp-2016-489, 2016
Manuscript under review for journal Atmos. Chem. Phys.
Published: 1 July 2016

Atmospheric Chemistry and Physics Discussions

The position and the main characteristics of the ships travelling in the central Mediterranean were derived from the MarineTraffic database (http://www.marinetraffic.com/), which provides the position of the ships with a high temporal resolution (about 3-5 minutes) by means of the Automatic Identification System (AIS).
Three classes of ships defined by the AIS classification were considered: all the ships, the merchant (i.e. cargo and tanker), and the fishing vessels. The merchant and fishing vessels are the most frequent ships in the Sicily Channel and the former are expected to produce the highest impact on the V concentration due to their higher emissions (http://ec.europa.eu/environment/archives/air/pdf/chapter2_ship_emissions.pdf).

3. Results

3.1. PM_{10} chemical composition at the two sites

The sea salt aerosol (SSA) component of PM_{10} was estimated as the sum of the sea salt (ss) fractions of Na^+, Mg^{2+}, Ca^{2+}, K^+, sulfate and chloride. Details on the calculation of sea salt Na^+ and Ca^{2+}, and non-sea salt (nss) fractions are reported in Marconi et al. (2014). The sea salt fractions of Mg^{2+}, Ca^{2+}, K^+, and sulphate were calculated from sea salt Na^+ ($ssNa^+$) by using the ratio of each component to Na^+ in bulk sea water: $Mg^{2+}/Na^+ = 0.129$, $Ca^{2+}/Na^+ = 0.038$, $K^+/Na^+ = 0.036$, $SO_4^{2-}/Na^+ = 0.253$ (Bowen, 1979). Chloride undergoes depletion processes during aging of sea spray, mainly due to exchange reactions with anthropic H_2SO_4 and HNO_3, leading to re-emission of HCl in the atmosphere. Thus, for chloride we use the measured chloride concentration instead of the one calculated from $ssNa^+$. Thus,

$$SSA = 1.46 *[ssNa^+] + [Cl^-]$$

The crustal component is calculated from Al, which represents 8.2% of the upper continental crust, UCC (Henderson and Henderson 2009). A previous study using an extensive data set at Lampedusa showed that the crustal content determined from the total Al was in very good agreement with calculations made from the sum of the metal oxides (Marconi et al., 2014). However, in this study we use measurements of the soluble Al concentration obtained by ICP-AES on the solution obtained with H_2O_2 and HNO_3 in microwave oven, instead of the total Al content. Therefore, in this work we underestimate the crustal contribution by about 30% (unpublished results). However, it must be emphasized that the crustal aerosol contribution was very low throughout the measurement campaign.

Figure 2 shows the time series of the main PM_{10} components at LMP and CGR. It must be noticed that an intense Mistral event occurred from 22nd June to 1st July. Mistral

Atmos. Chem. Phys. Discuss., doi:10.5194/acp-2016-489, 2016
Manuscript under review for journal Atmos. Chem. Phys.
Published: 1 July 2016

events are characterized by strong winds from the north-westerly sector, and often by subsiding air masses originating from the free troposphere. Thus, elevated values of SSA and low concentrations of other compounds are generally found during Mistral.
Average concentrations of PM_{10} and of the different aerosol components for the whole measurement campaign and for the non-Mistral conditions are reported in Table 1. The averages were calculated over a homogeneous dataset, i.e., only for the 12-hour intervals with observations at both sites.

The largest PM_{10} values were linked to elevated SSA during the Mistral event at both sites. PM_{10} is about two times larger at Capo Granitola than at Lampedusa. The PM_{10} measured during the campaign at Lampedusa was significantly smaller than its long-term average (31.5 µg/m^3; Marconi et al., 2014). No Saharan dust transport events occurred at low altitude in this period (e.g., Mailler et al., 2015), and the crustal aerosol contribution remained very low and almost constant at both sites (average < 1 µg/m^3 at LMP and around 3 µg/m^3 at CGR).

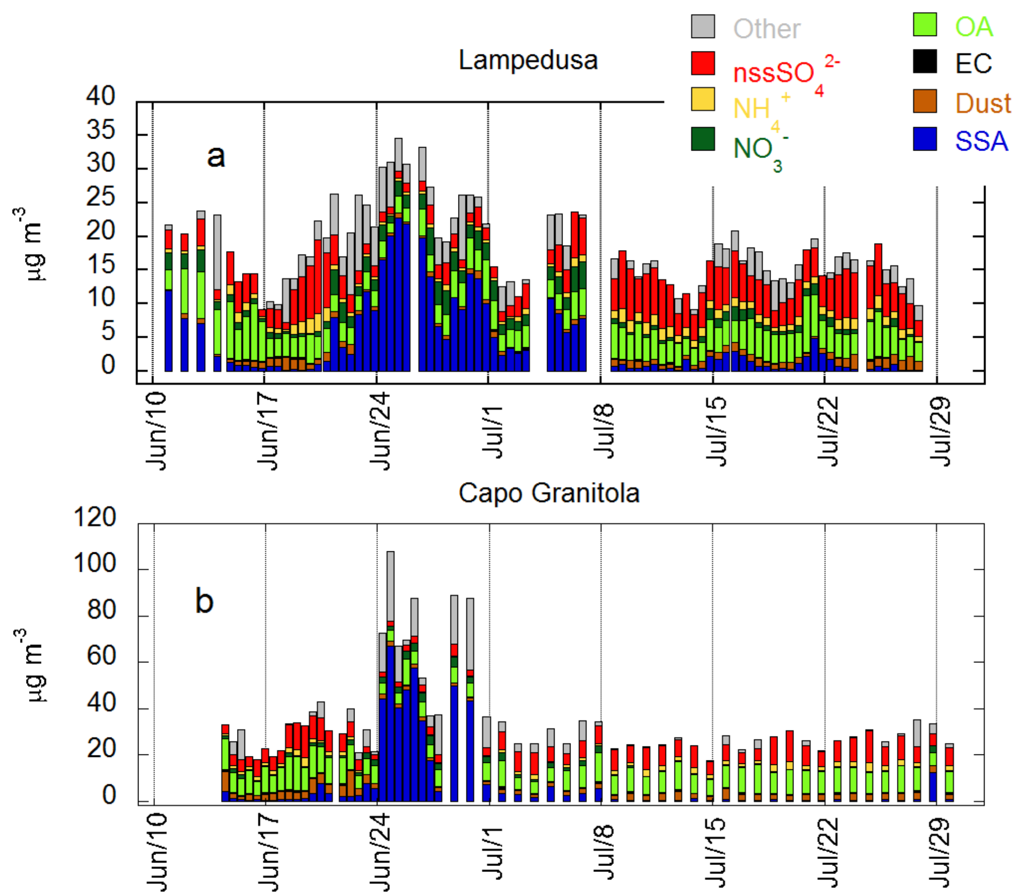

Atmos. Chem. Phys. Discuss., doi:10.5194/acp-2016-489, 2016
Manuscript under review for journal Atmos. Chem. Phys.
Published: 1 July 2016

Figure 2. Time series of the main aerosol components at LMP (plot a) and CGR (plot b). Note the different vertical scales of the graphs. For calculation of Organic Aerosol (OA) see text.

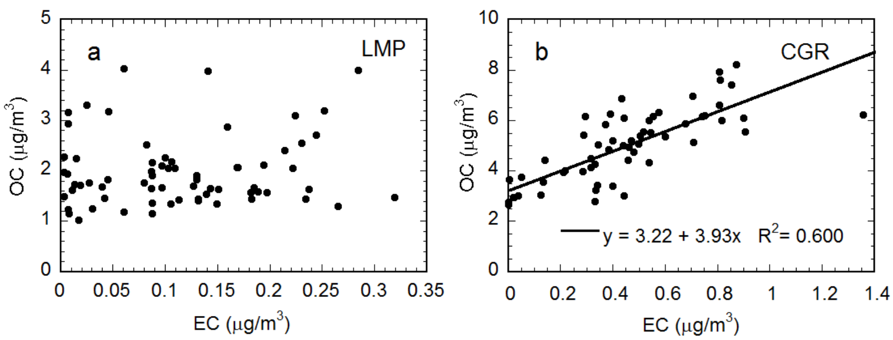

Figure 3. Scatter plot of OC vs. EC at LMP (plot a) and CGR (plot b). Note the different scales of the graphs.

SSA accounted for about 26% and 24% of PM_{10} at LMP and CGR, respectively. During the periods non influenced by the Mistral the SSA contribution was about 14% at LMP and 8% at CGR. Non-sea salt SO_4^{2-} was the most abundant among the secondary inorganic species.

Organic aerosol was the most abundant component at CGR, where its mean concentration was > 9 µg/m³ and represented 35% of PM_{10} in the days not characterized by Mistral. EC was about 4 times higher at CGR than at LMP.

Elemental carbon (EC) and organic carbon (OC) displayed a quite different behavior at the two sites. Figure 3 shows the behavior of OC versus EC at LMP and CGR. OC is correlated with EC (R^2=0.60; n =59) at CGR, suggesting a strong influence from carbon species primary sources, which are characterized by the simultaneous emission of EC and OC. At LMP, on the contrary, OC was not correlated with EC, indicating a strong impact of OC secondary and/or natural sources.

Atmos. Chem. Phys. Discuss., doi:10.5194/acp-2016-489, 2016
Manuscript under review for journal Atmos. Chem. Phys.
Published: 1 July 2016

Thus, we used a conversion factor of 1.8 (typical for urban background sites, Turpin and Lin, 2001) at CGR, and a conversion factor of 2.1 (typical for remote sites characterized by high impact of secondary sources, Turpin and Lin, 2001) at LMP to estimate the total organic aerosol (OA) amount from the measured values of OC. Once estimated OA with this method, the sum of the various species accounted to more than 85% of the measured mass at both sites. The unreconstructed mass could be due to an underestimation of OA from OC, or to the presence of bound water not removed by the desiccation procedure at 50% relative humidity (Tsyro, 2005; Canepari et al., 2013).

Figure 4 shows the combined evolution of $nssSO_4^{2-}$, OA, and V at CGR between 14 and 21 June, based on the 12-hour resolution data. As discussed above, OA was mainly due to inland primary sources, while V was expected to be mainly associated with ship emissions (Becagli et al., 2012). Non-sea salt SO_4^{2-} sources are expected to be present both on land and on sea. It is interesting to note the diurnal cycle at CGR in the period 14-18 June (Figure 4). The daily cycle is very likely related to the sea breeze regime which is expected to play a significant role at CGR, and a negligible role at LMP, due to the island small size.
In the days with dominant sea breeze regime, air masses are advected from the sea during daytime, and displayed low values of OA and elevated values of V. In nighttime, when land air masses were driven to the coast, OA was larger, and V lower than in daytime.

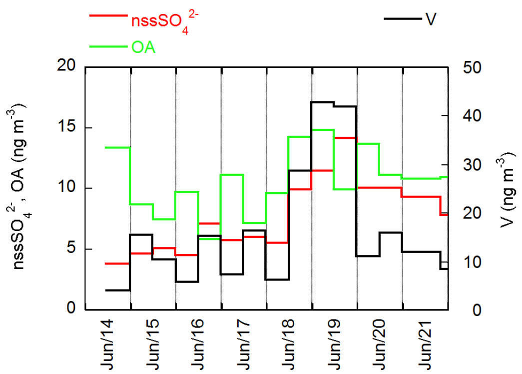

Figure 4. Time series of $nssSO_4^{2-}$, organic aerosol (OA), and V_{sol} at CGR.

3.1.1. Ship emission markers: V and Ni

Several studies focussed on the identification of specific tracers of shipping emissions (Viana et al., 2008; Becagli et al., 2012, Isakson et al., 2001, Hellebust et al., 2010).

Vanadium and Nickel are generally considered the best markers for this source because, after sulfur, they are the main impurities in heavy fuel oil (Agrawal et al., 2008a and b). The soluble fraction of these metals is even more representative for the ship source (Becagli et al., 2012).

Following Becagli et al. (2012), we used measurements of V and Ni soluble fractions (V_{sol} and Ni_{sol}, respectively). In the data set here considered the V_{sol} and Ni_{sol} ratio with respect to Al were always more than 10 times larger than for UCC, as expected for cases dominated by heavy oil combustions sources (ships, refineries, power plants, stainless steel production plants).

Figure 5 shows the time series of the V soluble fraction at LMP and CGR. Table 2 reports slope, correlation coefficient and number of samples of the linear correlation between V_{sol} and Ni_{sol}.

V_{sol} and Ni_{sol} are highly correlated, suggesting a common source. The obtained slope of the regression line (2.8-2.9, that increases to 3.0 for samples with V_{sol} >6 ng/m^3) is typical for heavy fuel oil combustion sources (Mazzei et al., 2008; Agrawal et al., 2008a and b, Viana et al. 2009; Pandolfi et al., 2011). The same value was found at Lampedusa by Becagli et al. (2012), considering data from 2004 to 2008. The behaviour of V, Ni, and their ratio are then representative of heavy fuel oil combustion. It is however difficult to distinguish V and Ni originating from power plants, refineries, or ship engines. Moreover, several refineries are present in Sicily (Siracusa, Gela, Milazzo) and in Sardinia (Cagliari) which may potentially influence the sampling sites.

A combination of methods is thus used in this study to unequivocally identify the ship source. The analysis is based on: additional chemical tracers, like the Rare Earth Elements, whose behaviour is specific for the refinery and the ship sources; high resolution back-trajectories, based on data from the high resolution regional model; information on the vertical mixing in the atmospheric boundary layer; coincidences between the high resolution back-trajectories and the position of different types of ships in the Sicily Channel.

3.1.2. Rare Earth elements

As discussed above, anthropic V and Ni originate from heavy oil combustion, and may be considered markers of the ship source only when other sources can be excluded. Few studies propose the use of lanthanoid elements (La to Lu) to distinguish refinery from ship emissions (Moreno et al. 2008). In particular, the ratio between the La and Ce concentrations (La/Ce ratio, hereafter LCR) has been used to identify specific sources. Shipping emissions are characterised by values of LCR between 0.6 and 0.8, similarly to the earth crust. Conversely, elevated values of LCR (from 1 to 5) are associated with emissions from refinery zeolitic fluid catalytic converter plants (Moreno et al., 2008).

Atmos. Chem. Phys. Discuss., doi:10.5194/acp-2016-489, 2016
Manuscript under review for journal Atmos. Chem. Phys.
Published: 1 July 2016

Atmospheric Chemistry and Physics
Discussions

LCR at LMP and CGR was generally around the value expected for UCC (Handerson and Handerson, 2009), also in events with high V_{sol} concentration (fig. 5).
At Capo Granitola LCR was >1 in 10% of the samples, and >2 in 3% of samples. At Lampedusa 24% of samples displayed LCR>1, and 8% LCR>2. Although during these days with LCR>1 the concentration of V_{sol} is usually low, a contribution of aerosol from refinery cannot be excluded.
The behaviour of V, La, and Ce is shown in a 3-component plot in figure 6. La and Ce were scaled in order to have the typical UCC composition in the central part of the plot. By comparison, the typical UCC composition and that of uncontaminated and La-contaminated (Refinery) Asian dust collected at Mauna Loa, Hawai'i by Olmez and Gordon (Olmez and Gordon, 1985) are also displayed in figure 6.
The data points from LMP and CGR are grouped in a region with elevated values of V, and marked different amounts of La and Ce with respect to V, differently from UCC and refineries.

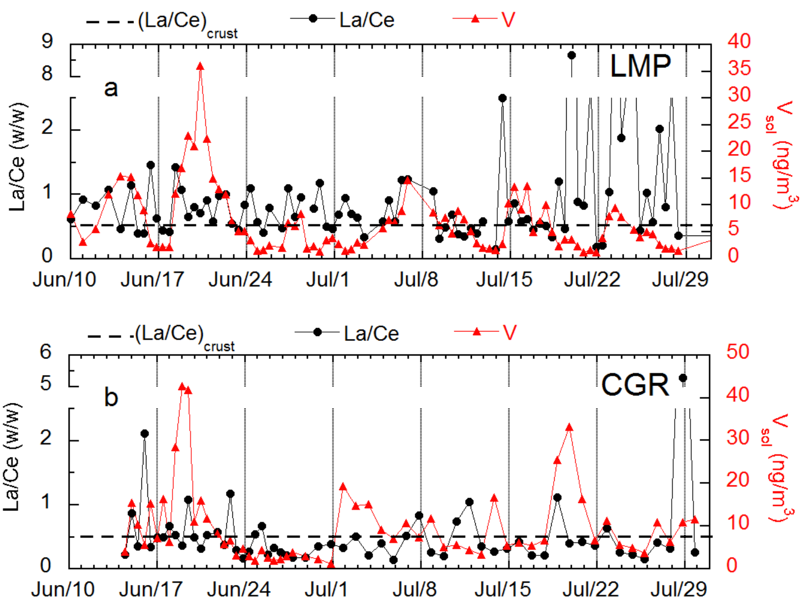

Figure 5. Time series of LCR and V at a), Lampedusa, and b), Capo Granitola. The horizontal black lines in each plot represent the LCR in the upper continental crust (0.5 w/w).

Atmos. Chem. Phys. Discuss., doi:10.5194/acp-2016-489, 2016
Manuscript under review for journal Atmos. Chem. Phys.
Published: 1 July 2016

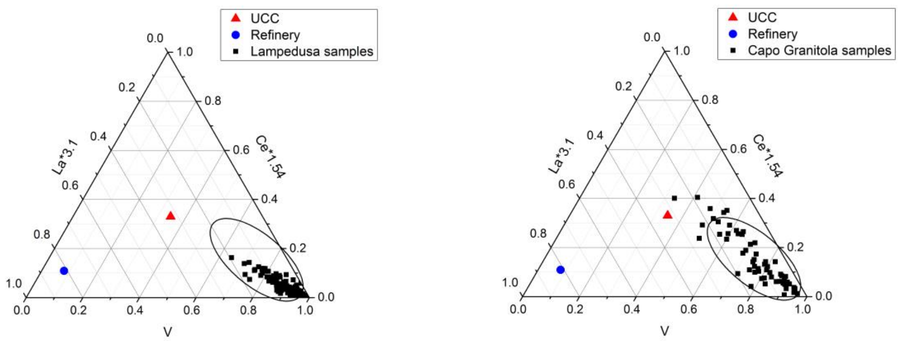

Figure 6. Three-component Ce-La-V plots for LMP (left) and CGR (right). The UCC composition is marked with a red triangle in the centre of the plots. The blue dot represents the composition of refinery-contaminated Asian dust (Olmez and Gordon, 1985). The black encircled area represents the ship emission composition.

The behaviour of the different chemical tracers support the conclusion that the V due to ship emissions is largely dominant in the PM_{10} measured at LMP and CGR during the measurement campaign. Thus, cases with elevated V can be used to identify cases with a large contribution from the ship source.

3.2. Trajectories and ship traffic

3.2.1 Origin of air masses during the campaign

All the trajectories arriving at LMP and CGR, calculated with the HYSPLIT model driven by the WRF meteorological fields (see Section 2.3), are shown in an aggregated way in Figure 7, where the trajectory frequency at each point of the computing grid is shown for the whole period (upper panels) and for the June 10^{th} – June 30^{th} interval (lower panels). While at LMP the trajectory frequency pattern is quite elongated in the NW-SE

Atmos. Chem. Phys. Discuss., doi:10.5194/acp-2016-489, 2016
Manuscript under review for journal Atmos. Chem. Phys.
Published: 1 July 2016

Atmospheric Chemistry and Physics
Discussions
Open Access

direction, at CGR trajectories are distributed over a wider range of directions, despite a general prevalence of northerly sectors. The predominance of air masses coming from the northwest is particularly evident in June (lower panels), when areas with trajectory frequencies exceeding 10% are found farther to the north, up to the Gulf of Lion.

During the first part of the campaign (June 2013), indeed, the synoptic situation was characterized by a "dipolar" sea level pressure anomaly pattern, with positive anomalies in the western Mediterranean and negative ones in the eastern part of the basin (Denjean et al., 2016). This situation induced stronger and more frequent than usual north-westerly winds (i.e. Mistral episodes, see Section 3.1) over the Sardinia and Sicily Channels.

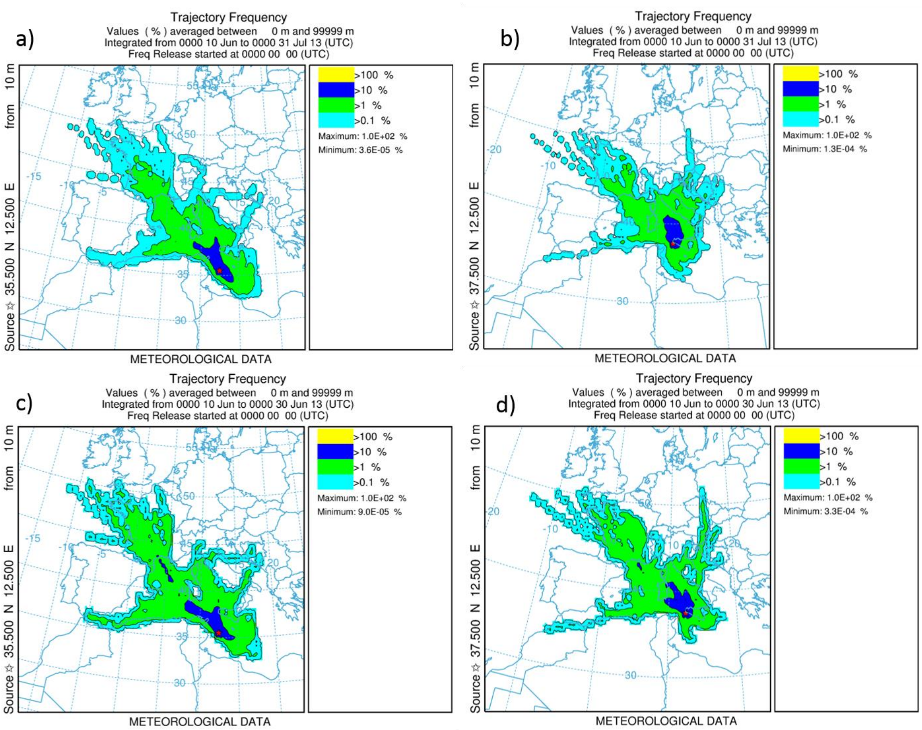

Figure 7. Trajectory frequency computed at each grid cell with starting points at LMP (panels a,c) and CGR (b,d). Upper panels show values averaged over the whole period of the campaign (10th June – 31st July 2013), while lower panels are relative to the June 10th –June 30th interval.

3.2.2 Ship traffic

To further investigate the mechanisms determining the V enhancement at the two sites we investigated the relationships among the amount of V, the back-trajectory pattern, the effective number of ships influencing the air mass, and the stability of the boundary layer in the ship source region (i.e., the Sicily Channel).
All back-trajectories arriving at LMP and CGR were considered and all trajectory-ship coincidences occurring within the last 36 hours before sampling were taken into account

It was assumed that the ship plume influenced the sampled air mass if:

- the trajectory passed at less than 15 km from the position of the ship
- the altitude of the air mass was lower than 500 m.

The total number of ships fulfilling these criteria was associated to each trajectory. The analysis was based on the available 1-hour time resolution meteorological fields (a ship influencing a trajectory was counted once every hour).
To further explore the impact of different types of ships, the analysis was carried out considering the following three ship categories: all the ships, the merchant (i.e. cargo and tanker), and the fishing vessels.

The atmospheric stability is also expected to play a large role in modulating the V amounts (Becagli et al. 2012). A temperature inversion, TI, index, was calculated based on the 3D atmospheric fields from the WRF model at three sites in the Sicily Channel. The temperature inversions have been used as a proxy to identify the periods characterized by a stable boundary layer. The three sites, A (37.2°N, 11.5°E), B (37.0°N, 12.4°E), and C (36.3°N, 13.3°E), were selected in the regions of most frequent ship passage and crossing with the trajectories from LMP and CGR. The TI index was calculated as the difference between the temperature at the altitude of the maximum T, and the surface T. A positive TI indicates an inversion, and the TI value provides an indication of the intensity of the inversion. Only positive values are considered in this analysis.

Figure 8 summarizes the results of this analysis. It shows the times series of the number of the ships influencing the trajectories arriving at LMP and CGR, respectively, and the corresponding measured values of V. Results are shown for the three classes of ships. The TI intensity is also shown.

In general, there is a rather good correspondence between the measured values of V and the number of ships encountered along the associated air mass trajectory at CGR. The correspondence is somewhat less evident at LMP. As discussed above, the V concentration is generally higher at CGR than at LMP. Part of this difference may be ascribed to the shorter distance between CGR and the main shipping route crossing the Sicily Channel with respect to Lampedusa, and the consequent larger number of encountered ships.

Atmos. Chem. Phys. Discuss., doi:10.5194/acp-2016-489, 2016
Manuscript under review for journal Atmos. Chem. Phys.
Published: 1 July 2016

Atmospheric Chemistry and Physics
Discussions
Open Access
EGU

The analysis of the event with elevated V concentration at both sites, between 18th and 21st June, provides further information to understand the link between the ship traffic and measured V concentration. This is the only event observed almost simultaneously at both stations. Maxima of V occurred between 19th and 20th June at CGR (about 42 ng/m^3), and on 21st June at LMP (36.1 ng/m^3). It is worth noting that similar concentrations were measured at CGR also around 18th-19th July, in conjunction with an increase in the number of merchant vessels.
On the other hand, the episode of 19th-21st June is the largest occurring at LMP, both for duration and V concentration. Especially at the beginning of the event, large values of V do not correspond with an increase of the number of ships along the air mass trajectories.

A possible explanation for this behavior is provided by the temporal evolution of TI in the Sicily Channel. The temperature inversion started to develop on 14 June, and gradually increased in intensity until 22 June; the TI persistence and progressive increase in intensity provided suitable conditions for the trapping of the ship plumes in the boundary layer, with a consequent build-up of the ship aerosol and V concentration. This process appears particularly efficient at CGR between 21 and 25 June.

A similar combined dependency on number of ships and TI appears also at LMP around 7 July. It is interesting to note that V seems to depend more directly on the number of merchant ships (see, e.g., the lack of V peaks on 17 June, 12 and 29 July at LMP, when the number of fishing vessels was high and the number of merchant ships was low) than on the total or the fishing ships.
Thus, the trajectory analysis carried out in combination with the available information on the ship tracks confirms that the ship emissions are the main responsible for the moderate and elevated values of V measured at LMP and CGR during the campaign. This analysis also clearly suggests that the boundary layer structure plays a very important role in determining the impact produced by the emissions. This simplified approach confirms the importance to carefully characterize the emission scenario and the meteorological conditions in studies on the impact of ships emissions on the air quality.

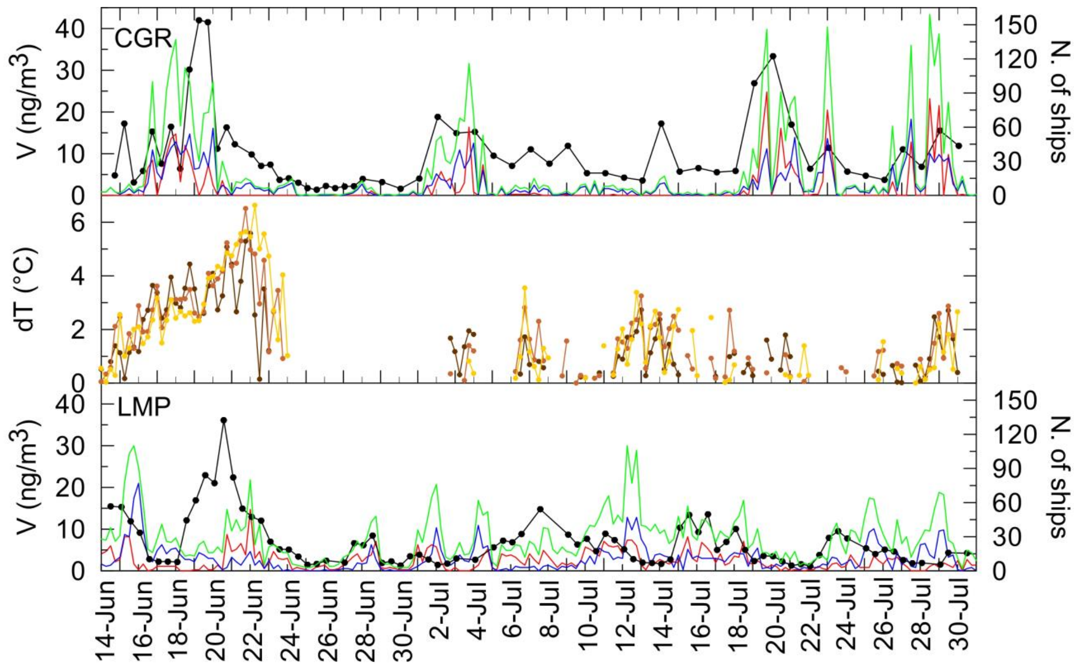

Figure 8. Time series of Vanadium concentration (black line with dots) and number of ships affecting the air masses sampled at CGR (upper panel) and LMP (lower panel). Green, red and blue lines indicate respectively the total number of ships, the number of merchant (i.e. cargo and tanker), and of fishing vessels. The time evolution of the temperature inversion index (dT in the figure) at three different locations in the Sicily Channels is shown in the middle panel; brown, red, and yellow curves show the behavior at sites A, B, and C (see text).

3.3. Sulfate, nitrate, and organic carbon from ships

SO_2 is one of the main species emitted in the ship plume in the gas phase (Agrawal et al., 2008a, b). SO_2 is produced through oxidation of the S contained as impurity in heavy fuel oil, and is an aerosol precursor.

A previous study performed at Lampedusa over 5 years (Becagli et al., 2012) showed that the behavior of non-sea salt sulfate is not directly correlated with V and Ni because several other SO_4^{2-} sources (anthropic, marine biogenic, crustal, volcanic) contribute to the non-sea salt sulfate in the Central Mediterranean Sea.

The same study suggests a lower limit of about 200 for the $nssSO_4^{2-}/V$ ratio for particles originating from heavy oil combustion at Lampedusa.

Atmos. Chem. Phys. Discuss., doi:10.5194/acp-2016-489, 2016
Manuscript under review for journal Atmos. Chem. Phys.
Published: 1 July 2016

Figure 9 shows $nssSO_4^{2-}/V$ versus V at LMP and CGR. At both sites $nssSO_4^{2-}/V$ decreases for increasing V and reaches a lower limit of about 200 at elevated values of V (> 15 ng/m^3). We assume that the ship emission is the dominant source of the sampled particles for these cases with elevated V. This implies that in these cases virtually all sulfate originated from the ship source, and the observed lower limit for $nssSO_4^{2-}/V$ can be considered the lower limit for the sulfate to V ratio in the ship plume.

We use a value of 200 in this work as a rough estimate of the sulfate to V ratio, based on the values obtained in the previous study and confirmed by the data set used in this study for two sites and reported in figure 9a and b. The $nssSO_4^{2-}/V$ limit values appears similar at LMP and CGR confirming the reliability of such values for the central Mediterranean Sea.

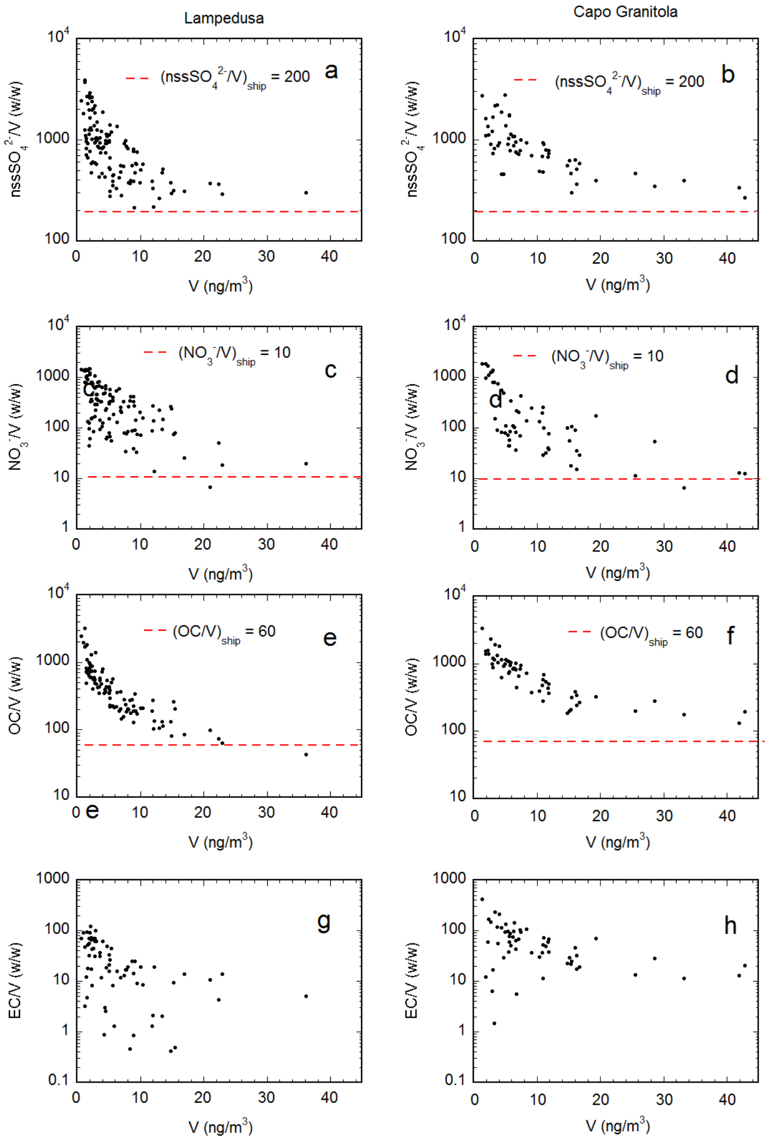

Figure 9. Scatter plots of $nssSO_4^{2-}/V$ (a and b), NO_3^-/V (c and d), OC/V (e and f) and EC/V (g and h) vs. V concentration at LMP (plots on the left) and CGR (plots on the right) sites. The dashed lines in the plot represent lower limits for the characteristic ratio in the ship plume.

NOx are among the main compounds emitted in gas phase acting as aerosol precursors. The photochemistry of NO_x leading to NO_3^- formation in the particulate phase is complex, especially in summer due to the presence of high amounts of OH radical (see e.g., Chen et al., 2005), and the NOx contribution to the particulate phase is not easy to be quantified.

Here we try to use the same approach used for sulfate for the determination of a lower limit for the NO_3^-/V ratio in the ship plume.

Figure 8 (plot c and d) shows the NO_3^-/V ratio versus V at the two sites. Similarly to sulfates, the NO_3^-/V ratio tends to a lower limit value (around 10 for V higher than 15 ng/m^3) at both sites. The NOx concentration is about two times larger than that of SO_2 in the ship plume close to the source (Agrawal et al 2008b) and lifetime of NOx is extremely low (1.8 hour during day and 6.5 hour during night, Chen et al., 2005). However, the NO_3^-/V limit ratio values is low compared to the limit ratio for SO_4^{2-}. It has to be considered that NO_3^- takes part in other photochemical atmospheric reactions that lead to its removal. Besides, the presence of HNO_3 in gas phase not neutralized by NH_3 or by sea salt could explain the low NO_3^-/nssSO_4^{2-} ratio in the aerosol. Indeed, the NO_3^- concentration measured at LMP and CGR is 4-6 times lower than that of nssSO_4^{2-} (table 1). Low amount of NO_3^- with respect to SO_4^{2-} from ship emissions are found in model simulations in Southern California (Dabdub, 2008). Indeed, Dabdub (2008) shows that the contribution to aerosol from ship emissions is 0.05% for NO_3^-, and 44% for SO_4^{2-}.

Elemental and Organic Carbon are also present in the ship plume (Shah et al., 2004). In particular, OC constitutes about 15-25% and EC is generally lower than 1% of the PM sampled at the plume of main ship engine powered by heavy fuel oil (Agrawal et al., 2008b).

Figure 9 shows EC/V and OC/V versus V at LMP and CGR. Similarly to sulfate and nitrate, OC/V decreases with increasing V and appears to reach a minimum value for V > 15 ng/m^3. As discussed in section 3.1, other OC sources in addition to ships are probably present at CGR even at high values of V. Thus, we assume that the OC/V value obtained at Lampedusa for V>15 ng/m^3 is representative of cases dominated by ship emissions, and this ratio is used to estimate the OC contribution due to ships at both sites.

The pattern of the ratio EC/V versus V is less clear; in particular, several very low values of EC/V appear also at small values of V. This result is unexpected because V and EC are both markers of the primary ship aerosol, but the data here presented seem to suggest that non negligible EC contributions from other sources were present, or that different fractionating effects acted during the transport.

3.4 Contribution of the ship aerosol to PM_{10}

With all the limitations above described, by using the lower limits for the ratios ($nssSO_4^{2-}$/V), (NO_3^-/V), and (OC/V) representative for ship aerosol it is possible to estimate the minimum contribution of $nssSO_4^{2-}$, NO_3^- and OC emitted by ships to the total budget of these component, and also to the total PM_{10} mass. It has to be noticed that the aerosol quantification obtained by this method is a rough estimate useful to constrain the ship aerosol contribution. In addition, due to possibly different meteorological conditions and photochemical activity, such values cannot be applied in general as they can vary spatially and seasonally.
The minimum ratio of each specie with respect to V, the minimum estimated contribution of ship emissions, for the average amount and for the maxima, to the total concentration of these species and to PM_{10}, are reported in Table 3. As previously discussed, the measured OC contribution is multiplied by 2.1 at LMP and by 1.8 at CGR to obtain the total organic aerosol contribution.

At LMP, the estimated minimum concentration of non-sea-salt sulfate from ship emissions was 1.3 μg/m^3, on average during this campaign. This value is lower than in the previous study by Becagli et al. (2012) obtained over a longer period (2004-2008). The relative contribution to the total sulfate is however similar here and in Becagli et al. (2012), suggesting a similar role of $nssSO_4^{2-}$ from ship emissions to the total $nssSO_4^{2-}$ budget. At CGR the minimum ship contribution to sulfate, averaged over the same time period, is higher than at LMP (2.0 μg/m^3), but this higher value corresponds to a lower contribution to the total $nssSO_4^{2-}$, confirming that other $nssSO_4^{2-}$ sources are important at CGR.
Marmer and Langmann (2005) estimate that ship emissions contribute by 50% to the total amount of $nssSO_4^{2-}$ in the Mediterranean. This value is larger than the one we derive (about 30%); the reader is however reminded that we estimate a lower limit for the ship contribution, useful to constrain the ship impact.
However, our data show that in cases with largest ship impact the $nssSO_4^{2-}$ from ship contributes at least by 66% and 75% to the total $nssSO_4^{2-}$ at LMP and CGR, respectively.
Ships appear to contribute by small fractions to the total budget of NO_3^-. As previously mentioned, the atmospheric chemistry of NO_3^- is complex and the contribution of nitrate from ship emission could be highly variable especially in the Mediterranean region where high amount of UV radiation and highly reactive radical species are present.
Organic aerosol from ships also contributes significantly to the total OA amount and to the total PM; in particular, at LMP at least about 92% of the total OA may be attributed to the ship source in the case with maximum ship impact.
By summing these three contributions, it is possible to estimate the total aerosol mass due to ship emissions, and its contribution to the total mass of PM_{10}. The lower limit for the ship contribution was 1.9 μg/m^3 and 2.8 μg/m^3, corresponding to 11% and 8.2% of PM_{10} at LMP and CGR, respectively.

These percent contributions are higher than the annual average for the Mediterranean Region estimated by Viana et al. (2014). It has to be considered that these authors used data from harbour or coastal sites, which are highly affected by other sources in addition to ships, and where gas-to-particle conversion is still at its initial phase. Moreover, the percentage reported in this study refers to the summer season, when the ship contribution in the Mediterranean region is higher (Becagli et al., 2012).

In cases with maximum ship impact, the estimated lower limit for the ship contribution was between 40% and 48% of the total PM_{10}.

Summary and conclusions

In this study, we investigate the impact of the ship emissions to PM_{10} on measurements made at two sites in the central Mediterranean. The main objectives of the study were to unambiguously identify the tracers of ship emissions in the sampled aerosol, and to obtain a lower limit for the produced impact.
The PM_{10} samples were collected in summer 2013, as a contribution to the Chemistry and Aerosol Mediterranean Experiment, in parallel at Lampedusa and at Capo Granitola, respectively South and North of the main shipping route through the Mediterranean.

The identification of aerosol originating from ships was based on an integrated analysis combining chemical analyses, calculations of backward trajectories using a high resolution regional model, and on tracking of ship traffic in the Mediterranean through the Automatic Identification System.

The main results of this study may be summarized as follows:

1. moderate and elevated values of V and Ni in the aerosol were unambiguously associated with the ship source; this attribution was based on:
    - the V to Ni ratio, which corresponds to what expected for heavy fuel oil combustion;
    - low amounts of La and Ce with respect to V, and La/Ce ratio similar to those in the UCC, which allowed to exclude power plants or refineries as sources significantly contributing to the observed aerosol;
    - coincidences between air mass trajectories and travelling ships;
2. in addition to travelling ships, also the planetary boundary layer vertical structure played an important role in determining the dispersion of aerosols from the ship source; temperature inversions appeared to be associated with elevated amounts of ship emissions tracers, suggesting that they favoured the build-up of aerosol concentration in the lowest atmospheric layers;

Atmos. Chem. Phys. Discuss., doi:10.5194/acp-2016-489, 2016
Manuscript under review for journal Atmos. Chem. Phys.
Published: 1 July 2016

3. merchant ships (cargo and tankers) appeared to produce a larger impact on the measured aerosol than fishing vessels;

4. lower limits for the ratios $nssSO_4^{2-}$/V, NO_3^-/V, and OC/V, identifying the ship-dominated emission cases, were derived from the observations. The lower limits are respectively 200, 10, and 40. These lower limits are expected to be season and site-dependent;

5. by using these ratios, the lower limits to the contribution of the ship source to $nssSO_4^{2-}$, NO_3^-, OA, and to PM_{10} during the measurement campaign were estimated. Ship emissions contributed by at least 30% to the total amount of sulfate, by at least 4-7% to the total amount of NO_3^-, and by at least 8-14% to the total amount of organic aerosol. All these contributions correspond at least to 11% of PM_{10} at LMP (1.9 $\mu g/m^3$), and about 8% of PM_{10} at CGR (2.8 $\mu g/m^3$). In cases with largest ship impact, ships contributed up to 12 $\mu g/m^3$ to PM_{10}, and by about 48% of PM_{10} at LMP and 40% at CGR.

Acknowledgements

Measurements at Lampedusa were partly supported by the Italian Ministry for University and Research through the NextData and Ritmare projects.
We thank the Institute for Coastal Marine Environment of the National Research Council (IAMC-CNR), for hosting the instruments at Capo Granitola. Thanks are due to MarineTraffic (www.marinetraffic.com) for providing the information on the ship traffic in the Sicily Channel.

Atmos. Chem. Phys. Discuss., doi:10.5194/acp-2016-489, 2016
Manuscript under review for journal Atmos. Chem. Phys.
Published: 1 July 2016

Table 1. Mean PM_{10} load and composition with the related standard deviation and percentage with respect to PM_{10} (in bracket) at Lampedusa and Capo Granitola. Mean, standard deviation and percentage are calculated on homogeneous data sets for both sites considering all the common sampling ("all data" columns) and excluding the mistral events ("Mistral excluded" columns).

	Lampedusa		**Capo Granitola**	
	All data	**Mistral excluded**	**All data**	**Mistral excluded**
PM_{10} (μg/m^3)	18.0±6.6	16.3±5.2	34.1±18.9	27.2±6.5
Sea Salt Aerosol (μg/m^3)	4.63±6.30 (25.7%)	2.33±3.21 (14.3%)	8.14±15.50 (23.9%)	2.12±6.51 (7.8%)
Crustal Aerosol (μg/m^3)	0.82±0.44 (4.6%)	0.90±0.43 (5.5%)	2.80±1.7 (8.2%)	3.02±1.75 (11.1%)
$nssSO_4^{2-}$ (μg/m^3)	3.95±2.28 (21.9%)	4.40±2.22 (27.0%)	6.78±3.08 (19.9%)	7.53±2.78 (27.7%)
NH_4^+ (μg/m^3)	0.98±0.56 (5.5%)	1.09±0.55 (6.7%)	1.48±0.94 (4.3%)	1.66±0.87 (6.1%)
NO_3^- (μg/m^3)	1.25±1.00 (7.0%)	1.02±0.02 (6.2%)	1.35±1.11 (4.0%)	1.01±0.82 (3.7%)
OA (μg/m^3)	3.86±1.56 (21.4%)	4.04±1.59 (24.8%)	9.02±2.52 (26.5%)	9.53±2.29 (35.0%)
EC (μg/m^3)	0.15±0.08 (0.8%)	0.15±0.08 (0.9%)	0.44±0.28 (1.3%)	0.51±0.26 (1.9%)
Unknown (μg/m^3)	2.52±3.26 (14.0%)	2.20±3.40 (13.5%)	4.11±7.78 (12.1%)	1.82±4.48 (6.7%)

Atmos. Chem. Phys. Discuss., doi:10.5194/acp-2016-489, 2016
Manuscript under review for journal Atmos. Chem. Phys.
Published: 1 July 2016

Table 2. Correlation parameters between V and Ni at LMP and CGR PM_{10} samples for all the samples and for samples with V concentration higher than 6 ng/m^3.

		Slope (± uncertainty)	**R^2**	**n.**
LMP	All data	2.94±0.03	0.986	124
	V_{sol} > 6ng/m^3	2.99±0.03	0.994	44
CGR	All data	2.82±0.08	0.950	59
	V_{sol} > 6ng/m^3	3.00±0.05	0.989	34

Table 3. Estimated minimum ratio of $nssSO_4^{2-}$, NO_3^-, OA with respect to V, minimum contribution of each species from ship emissions averaged over the considered time period and for the cases with highest ship impact of $nssSO_4^{2-}$, NO_3^-, OA and PM_{10} at LMP and CGR.

	$nssSO_4^{2-}$ ($(nssSO_4^{2-}/V)_{min}$=200)		**NO_3^-** ($(NO_3^-/V)_{min}$=10)		**OA** ($(OC/V)_{min}$=40)		**PM_{10}**	
	LMP	CGR	LMP	CGR	LMP	CGR	LMP	CGR
Average contribution μg/m^3 (%)	1.3 (33%)	2.0 (30%)	0.065 (4.5%)	0.10 (7.2%)	0.55 (14%)	0.72 (8.1%)	1.9 (11%)	2.8 (8.2 %)
Maximum contribution μg/m^3 (%)	7.2 (66%)	8.6 (75%)	0.36 (50%)	0.43 (80%)	3.0 (92%)	3.1 (21%)	10.6 (48%)	12.1 (40%)

References

Atmos. Chem. Phys. Discuss., doi:10.5194/acp-2016-489, 2016
Manuscript under review for journal Atmos. Chem. Phys.
Published: 1 July 2016

Atmospheric Chemistry and Physics
Discussions

Agrawal, H., Malloy, Q.G.J., Welch, W.A., Miller, J.W., Cocker, D.R.: In-use gaseous and particulate matter emissions from a modern ocean going container vessel. Atmos. Environ., 42, 5504−5510, 2008a.

Agrawal, H., Welch, W.A., Miller, J.W., Cocker, D.R.: Emission measurements from a crude oil tanker at sea. Environ. Sci. Technol., 42, 7098−7103, 2008b.

Artuso, F., P. Chamard, S. Piacentino, A. di Sarra, D. Meloni, F. Monteleone, D. Sferlazzo, and F. Thiery, Atmospheric methane in the Mediterranean: analysis of measurements at the island of Lampedusa during 1995-2005, Atmos. Environ., 41, 3877-3888, 2007.

Artuso, F., P. Chamard, S. Piacentino, D. M. Sferlazzo, L. De Silvestri, A. di Sarra, D. Meloni, F. Monteleone, Influence of transport and trends in atmospheric CO2 at Lampedusa, Atmos. Environ., 43, 3044–3051, 2009.

Ault, A. P., Gaston, C. J., Wang, Y., Dominguez, G., Thiemens, M. H., and Prather, K. A.: Characterization of the single particle mixing state of individual ship plume events measured at the port of los Angeles, Environ. Sci. Technol., 44, 1954–1961, 2010.

Becagli, S., L. Lazzara, F. Fani, C. Marchese, R. Traversi, M. Severi, A. di Sarra, D. Sferlazzo, S. Piacentino, C. Bommarito, U. Dayan, R. Udisti, Relationship between methanesulfonate (MS-) in atmospheric particulate and remotely sensed phytoplankton activity in oligo-mesotrophic Central Mediterranean Sea, Atmos. Environ., 79, 681-688, 2013.

Becagli, S., Sferlazzo, D. M., Pace, G., di Sarra, A., Bommarito, C., Calzolai, G., Ghedini, C., Lucarelli, F., Meloni, D., Monteleone, F., Severi, M., Traversi, R., and Udisti, R.: Evidence for heavy fuel oil combustion aerosols from chemical analyses at the island of Lampedusa: a possible large role of ships emissions in the Mediterranean, Atmos. Chem. Phys., 12, 3479–3492, doi:10.5194/acp-12-3479-2012, 2012.

Bove, M. C., Brotto, P., Calzolai, G., Cassola, F., Cavalli, F., Fermo, P., Hjorth, J., Massabò, D., Nava, S., Piazzalunga, A., Schembari, C., and Prati, P.: PM_{10} source apportionment applying PMF and chemical tracer analysis to ship-borne measurements in the Western Mediterranean, Atmos. Environ., 125, 140-151, http://dx.doi.org/10.1016/j.atmosenv.2015.11.009, 2016.

Bove, M. C., Brotto, P., Cassola, F., Cuccia, E., Massabò, D., Mazzino, A., Piazzalunga, A., and Prati, P.: An integrated PM2.5 source apportionment study: Positive Matrix Factorization vs. the Chemical Transport Model CAMx, Atmos. Environ., 94, 274–286, doi:10.1016/j.atmosenv.2014.05.039, 2014.

Bowen, H. J. M.: Environmental chemistry of the elements, Academic Press, 1979.

Calzolai, G., S. Nava, F. Lucarelli, M. Chiari, M. Giannoni, S. Becagli, R. Traversi, M. Marconi, D. Frosini, M. Severi, R. Udisti, A. di Sarra, G. Pace, D. Meloni, C. Bommarito, F. Monteleone, F. Anello, and D. M. Sferlazzo, Characterization of PM10 sources in the central Mediterranean, Atmos. Chem. Phys., 15, 13939–13955, 2015.

Canepari, S., Farao, C., Marconi, E., Giovannelli, C., and Perrino, C.:. Qualitative and quantitative determination of water in airborne particulate matter, Atmos. Chem. Phys., 13, 1193–1202, doi:10.5194/acp-13-1193-2013, 2013.

906 Cassola, F., Ferrari, F., Mazzino, A., and Miglietta, M. M.: The role of the sea on the flash floods events over Liguria (northwestern Italy), Geophys. Res. Lett., 43, doi:10.1002/2016GL068265, 2016.
909 Cesari, D., Genga, A., Ielpo, P., Siciliano, M., Mascolo, G., Grasso, F.M., Contini, D.: Source apportionment of PM2.5 in the harbour–industrial area of Brindisi (Italy): Identification and estimation of the contribution of in-port ship emissions. Sci. of the Total Environ., 497–498, 392–400, 2014.
913 Chen, G., Huey, G., Trainer, M.: An investigation of the chemistry of ship emission plumes during ITCT 2002. J. Geophys. Res. 110, D10S90, doi:10.1029/2004JD005236., 2005.
916 Coakley Jr., J. A. and Walsh, C. D.: Limits to the aerosol indirect radiative effect derived from observations of ship tracks, J. Atmos. Sci, 59, 668–680, 2002.
918 Contini, D., Gambaro, A., Belosi, F., Pieri, S.D., Cairns, W.R.L., Donateo, A., Zanotto, E., Citron, M.: The direct influence of ship traffic on atmospheric PM2.5, PM_{10} and PAH in Venice. J. of Environ. Management 92, 2119-2129, 2011.
921 Cooper, D.A.: Exhaust emissions from ships at berth. Atmos. Environ., 37, 3817−3830, 2003.
923 Corbett, J.J., Winebrake, J.J., Green, E.H., Kasibhatla, P., Eyring, V., and Lauer, A.: Mortality from Ship Emissions: A Global Assessment, Environ. Sci., Technol., 41, 8512–8518, doi:10.1021/es071686z, 2007.
926 Dabdub, D., Air quality impacts of ship emission in south coast air basin of California. Final report for State of California Air Resources Board Planning and Technical support division. 2008.
929 Denjean, C., Cassola, F., Mazzino, A., Triquet, S., Chevaillier, S., Grand, N., Bourrianne, T., Momboisse, G., Sellegri, K., Schwarzenbock, A., Freney, E., Mallet, M., and Formenti, P.: Size distribution and optical properties of mineral dust aerosols transported in the western Mediterranean, Atmos. Chem. Phys., 16, 1081-1104, doi:10.5194/acp-16-1081-2016, 2016.
934 Derwent, R., Stevenson, D. S., Doherty, R. M, Collins, W. J., Sanderson, M. G., Amann, M., and Dentener, F.: The contribution from ship emissions to air quality and acid deposition in Europe, Ambio, 34, 54–59, 2005.
937 Devasthale, A., Kr¨uuger, O., and Graßl, H.: Impact of ship emissions on cloud properties over coastal areas, Geophys. Res. Lett., 33, L02811, doi:10.1029/2005GL024470, 2006.
940 Diesch, J.M, Drewnick, F., Klimach, T., Borrmann, S.: Investigation of gaseous and particular emissions from various marine vessel types measured on the banks of the Elbe in Northern Germany. Atmos. Chem. and Phys. 13, 3603–3618, 2013.
943 di Sarra, A., C. Di Biagio, D. Meloni, F. Monteleone, G. Pace, S. Pugnaghi, and D. Sferlazzo: Shortwave and longwave radiative effects of the intense Saharan dust event of 25-26 March, 2010, at Lampedusa (Mediterranean sea), J. Geophys. Res., 116, D23209, doi: 10.1029/2011JD016238, 2011.
947 di Sarra, A., D. Sferlazzo, D. Meloni, F. Anello, C. Bommarito, S. Corradini, L. De Silvestri, T. Di Iorio, F. Monteleone, G. Pace, S. Piacentino, and S, Pugnaghi:

Atmos. Chem. Phys. Discuss., doi:10.5194/acp-2016-489, 2016
Manuscript under review for journal Atmos. Chem. Phys.
Published: 1 July 2016

Atmospheric Chemistry and Physics Discussions

Empirical correction of MFRSR aerosol optical depths for the aerosol forward scattering and development of a long-term integrated MFRSR-Cimel dataset at Lampedusa, Appl. Opt., 54, 2725-2737, 2015.

Donateo, A., E. Gregoris, A. Gambaro, E. Merico, R. Giua, A. Nocioni, D. Contini: Contribution of harbour activities and ship traffic to PM2.5, particle number concentrations and PAHs in a port city of the Mediterranean Sea (Italy), Environ Sci Pollut Res (2014) 21:9415–9429. DOI 10.1007/s11356-014-2849-0

Endresen, Ø., Sørg°ard, E., Sundet, J. K., Dalsøren, S. B., Isaksen, I. S. A., Berglen, T. F., and Gravir, G.: Emissions from international sea transportation and environmental impact, J. Geophys. Res., 108, 4560, doi:10.1029/2002JD002898, 2003.

Environmental Modeling Center: The GFS Atmospheric Model. NCEP Office Note 442. National Oceanic and Atmospheric Administration, 2003.

Eyring, V., Koehler, H.W., van Aardenne, J., and Lauer, A.: Emissions from international shipping: 1. The last 50 years, J. Geophys. Res., 110, D17305, doi:10.1029/2004JD005619, 2005.

Gariazzo, C., Papaleo, V., Pelliccioni, A., Calori, G., Radice, P., Tinarelli, G., Application of a Lagrangian particle model to assess the impact of harbour, industrial and urban activities on air quality in the Taranto area, Italy. Atmos. Environ. 41, 6432-6444, 2007.

Grewal, D., Haugstetter, H.: Capturing and sharing knowledge in supply chains in the maritime transport sector: critical issues. Maritime Policy & Management, 169-183. 2007.

Hellebust, S., Allanic, A., O'Connor, I.P., Jourdan, C., Healy, D., Sodeau, J.R.: Sources of ambient concentrations and chemical composition of PM2.5-0.1 in Cork Harbour, Ireland. Atmos. Res. 95, 136-149. 2010.

Henderson, P. and Henderson, G. M.: The Cambridge Handbook of Earth Science Data, Cambridge, University Press, Cambridge, 42–44, 2009.

Isakson, J., Persson, T.A., Lindgren, E.S.: Identification and assessment of ship emissions and their effects in the harbour of Goteborg, Sweden. Atmos. Environ. 35, 3659-3666. 2001.

Jonsson, A.M, Westerlund, J., Hallquist, M.: Size-resolved particle emission factors for individual ships. Geophys. Res. Let., 38, L13809. DOI: 10.1029/2011GL047672, 2011.

Kouvarakis, G., Tsigaridis, K., Kanakidou, M., and Mihalopous, N.: Temporal variations of surface regional background ozone over Crete Island in the southeast Mediterranean, J. Geophys. Res., 105, 4399–4407, 2000.

Lauer, A., Eyring, V., Hendricks, J., J¨ockel, P., and Lohmann, U.: Global model simulations of the impact of ocean-going ships on aerosols, clouds, and the radiation budget, Atmos. Chem. Phys., 7, 5061–5079, doi:10.5194/acp-7-5061-2007, 2007.

Li, Z. and Aneja, V. P.: Regional analysis of cloud chemistry at high elevations in the eastern United States, Atmos. Environ., 26A, 2001–2017, 1992.

Atmos. Chem. Phys. Discuss., doi:10.5194/acp-2016-489, 2016
Manuscript under review for journal Atmos. Chem. Phys.
Published: 1 July 2016

Lloyd's Register Engineering Services, 1995. Marine Exhaust Emissions Research Programme, London. pp. 63.

Lucarelli, F., Nava, S., Calzolai, G., Chiari, M., Udisti, R., and Marino, F.: Is PIXE still a useful technique for the analysis of atmospheric aerosols? The LABEC experience, X-Ray Spectrometry, 40, 162–167, 2011.

Lyyränen, J., Jokiniemi, J., Kauppinen, E.I., Joutsensaari, J.: Aerosol characterisation in medium-speed diesel engines operating with heavy fuel oils. J. Aerosol Sci. 30, 771−784, 1999.

Mailler S., L. Menut, A. G. di Sarra, S. Becagli, T. Di Iorio, B. Bessagnet, R. Briant, P. Formenti, J.-F. Doussin, J. L. Gómez-Amo, M. Mallet, G. Rea, G. Siour, D. M. Sferlazzo, R. Traversi, R. Udisti, and S. Turquety: On the radiative impact of aerosols on photolysis rates: comparison of simulations and observations in the Lampedusa island during the ChArMEx/ADRIMED campaign. Atmos. Chem. Phys., 16, 1219–1244, doi:10.5194/acp-16-1219-2016, 2016.

Mallet, M., Dulac, F., Formenti, P., Nabat, P., Sciare, J., Roberts, G., Pelon, J., Ancellet, G., Tanré, D., Parol, F., Denjean, C., Brogniez, G., di Sarra, A., Alados-Arboledas, L., Arndt, J., Auriol, F., Blarel, L., Bourrianne, T., Chazette, P., Chevaillier, S., Claeys, M., D'Anna, B., Derimian, Y., Desboeufs, K., Di Iorio, T., Doussin, J.-F., Durand, P., Féron, A., Freney, E., Gaimoz, C., Goloub, P., Gómez-Amo, J. L., Granados-Muñoz, M. J., Grand, N., Hamonou, E., Jankowiak, I., Jeannot, M., Léon, J.-F., Maillé, M., Mailler, S., Meloni, D., Menut, L., Momboisse, G., Nicolas, J., Podvin, T., Pont, V., Rea, G., Renard, J.-B., Roblou, L., Schepanski, K., Schwarzenboeck, A., Sellegri, K., Sicard, M., Solmon, F., Somot, S., Torres, B., Totems, J., Triquet, S., Verdier, N., Verwaerde, C., Waquet, F., Wenger, J., and Zapf, P.: Overview of the Chemistry-Aerosol Mediterranean Experiment/Aerosol Direct Radiative Forcing on the Mediterranean Climate (ChArMEx/ADRIMED) summer 2013 campaign, Atmos. Chem. Phys., 16, 455-504, doi:10.5194/acp-16-455-2016, 2016.

Marconi, M., Sferlazzo, D.M., Becagli, S., Bommarito, C., Calzolai, G., Chiari, M., di Sarra A., Ghedini, C., Gómez-Amo, J.L., Lucarelli F., Meloni D., Monteleone F., Nava S., Pace G., Piacentino S., Rugi F., Severi M., Traversi R., and Udisti R.: Saharan dust aerosol over the central Mediterranean Sea: PM_{10} chemical composition and concentration versus optical columnar measurements Atmos. Chem. Phys., 14, 2039–2054, 2014.

Marmer, E. and Langmann, B.: Impact of ship emissions on Mediterranean summertime pollution and climate: A regional model study, Atmos. Environ., 39, 4659–4669, 2005.

Marmer, E., Dentener, F., Aardenne, J.V., Cavalli, F., Vignati, E., Velchev, K., Hjorth, J.,Moldanová, J., Fridell, E., Popovicheva, O., Demirdjian, B., Tishkova, V., Faccinetto, A., Focsa, C.: Characterisation of particulate matter and gaseous emissions from a large ship diesel engine. Atmos. Environ., 43, 2632−2641, 2009.

Mazzei F., D'Alessandro, A., Lucarelli, F., Nava, S., Prati, P., Valli, G., and Vecchi R.: Characterization of particulate matter sources in an urban environment. Sci. of Tot. Environ., 401, 81–89, 2008.

Atmos. Chem. Phys. Discuss., doi:10.5194/acp-2016-489, 2016
Manuscript under review for journal Atmos. Chem. Phys.
Published: 1 July 2016

Atmospheric Chemistry and Physics
Open Access
Discussions

Meloni, D., A. di Sarra, J. R. Herman, F. Monteleone, and S. Piacentino, Comparison of ground-based and TOMS erythemal UV doses at the island of Lampedusa in the period 1998-2003: Role of tropospheric aerosols, J. Geophys. Res., 110, D01202, doi: 10.1029/2004JD005283, 2005.

Meloni, D., C. Di Biagio, A. di Sarra, F. Monteleone, G. Pace, and D. M. Sferlazzo, Accounting for the solar radiation influence on downward longwave irradiance measurements by pyrgeometers, J. Atmos. Oceanic Technol., 29, 1629-1643, 2012.

Meloni, D., W. Junkermann, A. di Sarra, M. Cacciani, L. De Silvestri, T. Di Iorio , V. Estellés, J. L. Gómez-Amo, G. Pace, and D. M. Sferlazzo: Altitude-resolved shortwave and longwave radiative effects of desert dust in the Mediterranean during the GAMARF campaign: indications of a net daily cooling in the dust layer, J. Geophys. Res. Atmos., 120, 3386-3407, doi: 10.1002/2014JD022312, 2015.

Mentaschi, L., Besio, G., Cassola, F., and Mazzino, A.: Performance evaluation of WavewatchIII in the Mediterranean Sea, Ocean Model., 90, 82–94, doi:10.1016/j.ocemod.2015.04.003, 2015.

Micco, A., Pérez, N.: Maritime transport costs and port efficiency. In: Bank, I.-A.D. (Ed.), Inter-american Development Bank, Santiago de Chile, p. 50. 2001.

Moldanová, J., Fridell, E., Popovicheva, O., Demirdjian, B., Tishkova, V., Faccinetto, A., Focsa, C. Characterisation of particulate matter and gaseous emissions from a large ship diesel engine. Atmos. Environ. 2009, 43, 2632−2641.

Moreno, T., Querol, X., Alastuey, A., Pey, J. Cruzminguillon, M., Perez, N., Bernabe, R., Blanco, S. Cardenas, B., Gibbons, W., :Lanthanoid geochemistry of urban atmospheric particulate matter, Environ. Sci. Technol. 42, 6502–6507, 2008.

Murphy, S., Agrawal, H., Sorooshian, A., Padró, L.T., Gates, H., Hersey, S., Welch, W. A., Jung, H., Miller, J. W., Cocker, D.R. III, Nenes, A., Jonsson, H.H., Flagan, R.C., Seinfeld, J.H.: Comprehensive simultaneous shipboard and airborne characterization of exhaust from a modern container ship at sea. Environ. Sci. Technol. 43, 4626−4640, 2009.

Olmez, I., Gordon, G.E.: Rare earths: Atmospheric signatures for oil-fired power plants and refineries. Science, 6, 966–968, 1985.

Pandolfi, M., Gonzalez-Castanedo, Y., Alastuey, A., Rosa, J.d.l., Mantilla, E., Campa, A.S.d.l., Querol, X., Pey, J., Amato, F., Moreno, T., Source apportionment of PM_{10} and PM2.5 at multiple sites in the strait of Gibraltar by PMF: impact of shipping emissions. Environ. Sci. and Pollution Res. 18, 260-269, 2011.

Schembari, C., Bove, M. C., Cuccia, E., Cavalli, F., Hjorth, J., Massabò, D., Nava, S., Udisti, R., and Prati, P.: Source apportionment of PM10 in the Western Mediterranean based on observations from a cruise ship. Atmospheric Environment 98, 510-518, 2014.

Shah, S.D., Cocker, D.R., Miller, J.W., Norbeck, J.M.: Emission rates of particulate matter and elemental and organic carbon from in-use diesel engines. Environ. Sci. Technol., 38, 2544–2550, 2004.

Atmos. Chem. Phys. Discuss., doi:10.5194/acp-2016-489, 2016
Manuscript under review for journal Atmos. Chem. Phys.
Published: 1 July 2016

Sippula, O., Hokkinen, J., Puustinen, H., Yli-Piril¨a, P., and Jokiniemi J: Comparison of particle emissions from small heavy fuel oil and wood-fired boilers. Atmos. Environ., 43, 4855–4864, 2009.

Sippula, O., Stengel, B., Sklorz, M., Streibel, T., Rabe, R., Orasche, J., Lintelmann, J., Michalke, B., Abbaszade, G., Radischat, C., Gröger, T., Schnelle-Kreis, J., Harndorf, H., and Zimmermann R.: Particle emissions from a marine engine: chemical composition and aromatic emission profiles under various operating conditions. Environ. Sci. Technol., 48, 11721−11729, 2014.

Skamarock, W. C., Klemp, J. B., Dudhia, J., Gill, D. O., Barker, D. M., Huang, X. Z., Wang, W., and Powers, J. G.: A Description of the Advanced Research WRF Version 3. Technical report. Mesoscale and Microscale Meteorology Division, NCAR, Boulder, Colorado, 2008.

Stein, A. F., Draxler, R. R, Rolph, G. D., Stunder, B. J. B., Cohen, M. D., and Ngan, F.: NOAA's HYSPLIT atmospheric transport and dispersion modeling system, Bull. Amer. Meteor. Soc., 96, 2059-2077, http://dx.doi.org/10.1175/BAMS-D-14-00110.1, 2015.

Stern, N.,:The Economics of Climate Change: The Stern Review. Cambridge and New York, Cambridge University press. 2007.

Trozzi, C., Vaccaro, R., Nicolo, L.: Air pollutants emissions estimate from maritime traffic in the Italian harbours of Venice and Piombino. Sci. of the Tot. Environ., 169, 257–263, 1995.

Tsyro S. G.: To what extent can aerosol water explain the discrepancy between model calculated and gravimetric PM_{10} and $PM_{2.5}$?. Atmos. Chem. Phys., 5, 515–532, 2005. www.atmos-chem-phys.org/acp/5/515/SRef-ID: 1680-7324/acp/2005-5-515.

Turpin, B.J. and Lim H.J.: Species Contributions to PM2.5 Mass Concentrations: Revisting Common Assumptions for Estimating Organic Mass. Aerosol Sci. Technol. 35: 602–610, 2001.

Viana, M., Amato, F., Alastuey, A., Querol, X., Moreno, T., Santos, S.G.D., Herce, M.D., Fernández-Patier, R.: Chemical tracers of particulate emissions from commercial shipping. Environ. Sci. and Tech. 43, 7472-7477, 2009.

Viana, M., Hammingh, P., Colette, A., Querol, X., Degraeuwe, B., de Vlieger, I., van Aardenne, J.: Impact of maritime transport emissions on coastal air quality in Europe, Atmos. Environ., 90 96-105, 2014.

Viana, M., Kuhlbusch, T.A.J., Querol, X., Alastuey, A., Harrison, R.M., Hopke, P.K., Winiwarter, W., Vallius, M., Szidat, S., Prévôt, A.S.H., Hueglin, C., Bloemen, H., Wåhlin, P., Vecchi, R., Miranda, A.I., Kasper-Giebl, A., Maenhaut, W., Hitzenberger, R.: Source apportionment of particulate matter in Europe: a review of methods and results. J. of Aer. Sci., 39, 827-849, 2008.

World Health Organization (WHO): Health Effects of Particulate Matter, Policy Implications for Countries in Eastern Europe, Caucasus and Central Asia, Regional office for Europe, Copenhagen, Denmark, 2013.

Wu, C., Huang, X. H. H., Ng, W. M., Griffith, S. M., and Yu, J. Z.: Inter-comparison of NIOSH and IMPROVE protocols for OC and EC determination: Implications for inter-

Atmos. Chem. Phys. Discuss., doi:10.5194/acp-2016-489, 2016
Manuscript under review for journal Atmos. Chem. Phys.
Published: 1 July 2016

Atmospheric Chemistry and Physics Discussions
Open Access

protocol data conversion, Atmos. Meas. Tech. Discuss., doi:10.5194/amt-2016-116, in review, 2016